

Electron–plasmon relaxation in quantum wells with inverted subband occupation

Mikhail V. Kisin

Department of Electrical Engineering, State University of New York at Stony Brook, Stony Brook, New York 11794-2350

Michael A. Stroscio

U.S. Army Research Office, P.O. Box 12211, Research Triangle Park, North Carolina 27709-2211

Gregory Belenky^{a)} and Serge Luryi

Department of Electrical Engineering, State University of New York at Stony Brook, Stony Brook, New York 11794-2350

(Received 1 July 1998; accepted for publication 6 August 1998)

We have considered the electron-plasmon interaction and intersubband resonance screening in a quantum well with inverted subband occupation. We show that in such a system the intersubband plasmon emission leads to an efficient deexcitation of the nonequilibrium initial state and raises the occupation of states at the lower-subband bottom. Downshift and resonance narrowing of the intersubband optical emission spectra are obtained and shown to be influenced by the process of intersubband plasmon excitation. © 1998 American Institute of Physics.

[S0003-6951(98)01841-5]

Relaxation of nonequilibrium charge carriers is important for the performance of many electron heterostructure devices.^{1–3} At low sheet electron concentrations $N_s \leq 10^{12} \text{ cm}^{-2}$, the intrasubband relaxation in A_3B_5 heterostructures is determined basically by polar optical phonon and intrasubband–plasmon scattering processes, which become comparable at the level of electron concentration $N_s \approx 10^{11} \text{ cm}^{-2}$.¹ In laser heterostructures designed for optical transitions in the range $\hbar\omega \approx 150\text{--}300 \text{ meV}$ (Ref. 9), the relevant energy quanta $\hbar\omega_{\text{ph}}$ and $\hbar\omega_{\text{pl}}^{(11)}$, are small compared with the subband separation Δ_{21} , so that nonequilibrium electrons entering the first subband after intersubband 2–1 phonon-emission transitions must subsequently cascade down the first subband emitting the optical phonons and low-energy intrasubband plasmons. The high-energy intersubband plasmon mode, $\omega_{\text{pl}}^{(12)}$, being characterized by an antisymmetric potential distribution, could participate in the intersubband relaxation causing electron intersubband 2–1 transitions with a small momentum transfer. However, under the condition of Fermi filling of the first subband states, this kind of transition becomes possible only for high-energy electrons in the second subband because of the upshift of the energy of the intersubband collective excitations (plasmons)^{4–8}

$$\hbar\omega_{\text{pl}}^{(12)}(q) \approx \Delta_{21} + \delta_q, \quad \delta_q = \frac{e^2 N_s S}{\kappa_0 \kappa} [1 + O(qa)]. \quad (1)$$

Here, δ_q and S are, respectively, the depolarization shift of the intersubband excitation energy and depolarization integral,^{4,5} and κ is the dielectric constant. As a result, for electrons injected into the bottom of the second subband the plasmon-assisted intersubband relaxation is negligible.

The above picture of the relaxation process has been developed for the normal ordering of subband filling when most of electrons occupy the lower subband states, $N_s \approx n_1$. Operation of the quantum cascade laser (QCL)^{9,10} requires a nonequilibrium state of the active quantum well with a significant population in the upper subband, $N_s = n_1 + n_2$, including the situation with inverted subband occupation, $n_2 > n_1$. In this letter we demonstrate that the inverted order of subband occupation results in an effective relaxation mechanism for nonequilibrium electrons in the lower subband due to scattering by intersubband plasmon excitations of the upper-subband electrons. In contrast to the cascade relaxation by phonons and intrasubband plasmons, this one-step scattering process efficiently fills the lower-subband bottom and should be taken into consideration if one is interested in the realization of a high-gain QCL in the low-concentration regime.^{9,10}

We restrict ourselves to the two lowest parabolic subbands characterized by a Fermi-distributed population in the upper subband $N_s \approx n_2$ with the Fermi wave-vector k_F and Fermi energy ϵ_F . The intersubband plasmon potential $\varphi_{\text{pl}}^{(21)}(z, \mathbf{r}, t) = \varphi_{21}(z) e^{i\mathbf{q}\mathbf{r}} \cos \omega t$ causes polarization of the electronic system in the second subband corresponding to the admixture of lower-energy states $\psi_1(z)$ from the first subband to the occupied second-subband states $\psi_2(z)$. Using this induced charge distribution as a source in Poisson's equation⁴ we easily determine the intersubband plasmon energy $\hbar\omega_{\text{pl}}^{(21)}(q) \approx \Delta_{21} - \delta_q$. This quantum turns out to be smaller than $\hbar\omega_{\text{pl}}^{(12)}$ due to the positive sign of the electric-field energy, which is a part of the energy of the collective intersubband excitation. In contrast to the system with normal subband occupation [Fig. 1(a)], where the intersubband plasmon excitation raises the ground-state-energy E_0 by intersubband plasmon quantum, the polarization process (2) results in the *lowering* of the energy of the initial nonequi-

^{a)}Electronic mail: garik@sbee.sunysb.edu

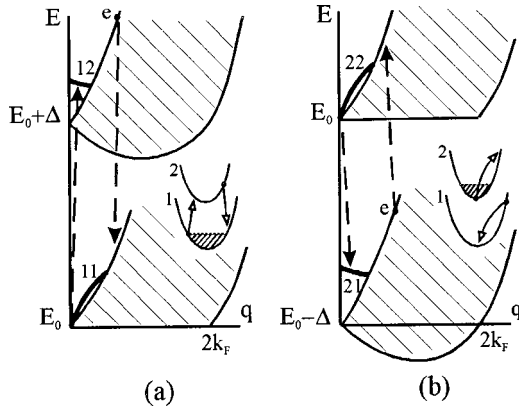


FIG. 1. Spectrum of electron excitation in a two-subband system with normal (a) and inverted (b) ordering of subband occupation. The continuum single-particle excitations of the initial-state E_0 is represented by shaded regions and the dispersions of intrasubband (11,22) and intersubband (12,21) collective excitations are shown by heavy solid lines. Dashed lines illustrate the scattering of an external electron (e) by intersubband plasmon. In the insets we show electron–electron scattering events, which are analogous to the electron–plasmon processes but are ineffective due to electron wave-function orthogonality (a) or large momentum transfer (b) (Ref. 3).

librium state [Fig. 1(b)]. As a result, the scattering process with intersubband plasmon emission in the inverted system must include the intersubband 1–2 electron transition associated with the absorption of the deexcitation energy $\hbar\omega_{\text{pl}}^{(21)}$. In accordance with the random phase approximation (RPA), the state of the inverted system with one excited intersubband plasmon can be represented as $|E_0 - \hbar\omega_{\text{pl}}^{(21)}(q)\rangle = \Sigma F(k)\hat{c}_{1,\mathbf{k}+\mathbf{q}}^+\hat{c}_{2,\mathbf{k}}|E_0\rangle$. The expectation value of the first-subband number operator in this state is then $\langle\hat{c}_{1,\mathbf{k}}^+\hat{c}_{1,\mathbf{k}}\rangle = |F(\mathbf{k}+\mathbf{q})|^2$, where the form-factor $F(k)$ obeys the normalization condition $\Sigma|F(k)|^2 = 1$. This implies an effective increase of the first subband occupation by one electron. Since $q \ll k_F$, this process fills the bottom states of the first subband—to a good approximation uniformly.

Following Refs. 9 and 10, we suppose the depopulation of the first subband to be fast tunneling events, $\tau_{1\text{out}} \ll \tau_{\text{ph}}^{(21)}$. Then, in a steady-state, one has $n_1 \approx n_2 \tau_{1\text{out}} / \tau_{\text{ph}}^{(21)} \ll n_2$, hence, the electron–plasmon scattering rates are determined essentially by the electron concentration in the second subband. The balance equation for the electrons occupying the bottom of the first subband (with partial concentration n_0) can be written in the form

$$\frac{m}{\pi\hbar^2} \int_{\epsilon_{\text{th}}}^{\Delta - \hbar\omega_{\text{ph}}} d\epsilon_1 \frac{f(\epsilon_1)}{\tau_{\text{pl}}^{(21)}(\epsilon_1)} = \frac{n_0}{\tau_{1\text{out}}}, \quad (2)$$

where $f(\epsilon_1)$ is the electron distribution function in the first subband, normalized as

$$\frac{m}{\pi\hbar^2} \int_{\epsilon_F}^{\Delta - \hbar\omega_{\text{ph}}} d\epsilon_1 f(\epsilon_1) = n_1 - n_0, \quad (3)$$

$$f(\epsilon_1 < \epsilon_F) = f_0 \approx \frac{\pi\hbar^2 n_0}{m\epsilon_F},$$

and $1/\tau_{\text{pl}}^{(21)}$ is the electron scattering rate by intersubband plasmons, $\omega_{\text{pl}}^{(21)}$. In the high-energy region, $\epsilon_F < \epsilon_1 < \Delta_{21}$, the distribution function $f(\epsilon_1)$ is established by optical phonon and intrasubband–plasmon–cascade emission and can be approximated by the simple expression¹⁰

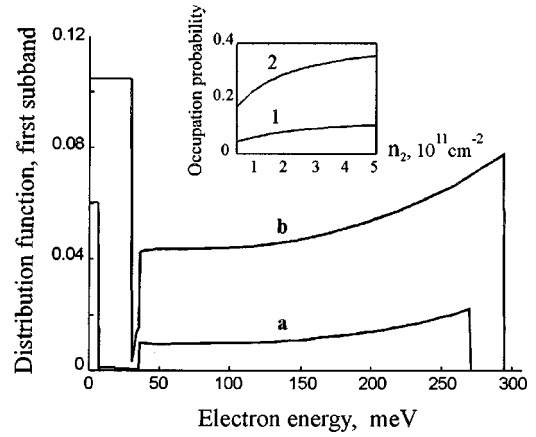


FIG. 2. Approximate nonequilibrium distribution function for electrons in the first subband for subband depopulation time $\tau_{1\text{out}} = 1$ ps and two values of electron concentration n_2 : (a) $1 \times 10^{11} \text{ cm}^{-2}$, (b) $5 \times 10^{11} \text{ cm}^{-2}$. The inset shows the occupation probability for electron states near the first subband bottom as a function of electron concentration n_2 for two different values of $\tau_{1\text{out}}$ (in ps).

$$f(\epsilon_1) \propto \exp\left(-\frac{\Delta_{21}\hbar\omega_{\text{ph}} - \epsilon_1}{W_{\text{cc}}\tau_{1\text{out}}}\right), \quad (4)$$

where $W_{\text{cc}} = W_{\text{ph}}^{(11)} + W_{\text{pl}}^{(11)}$ is the total cascade cooling rate for 1–1 intersubband relaxation processes. For an exemplary calculation, we consider an infinitely deep quantum well with subband energy separation $\Delta_{21} = 300$ meV and width $a = 4$ nm. All material parameters correspond to $\text{Ga}_{0.47}\text{In}_{0.53}\text{As}$. The scattering rates, $1/\tau_{\text{pl,ph}}$ have been calculated for $T = 0$ K by the standard method using the dielectric continuum model.¹¹ To simplify the model, the phonon spectrum has been approximated by bulk phonons, neglecting phonon confinement effect.^{1,12} The electron concentration range is chosen to be $5 \times 10^{10} - 5 \times 10^{11} \text{ cm}^{-2}$, which is typical for the QCL.⁹ Phonon–plasmon coupling becomes important at higher concentration level $N_s \geq 10^{12} \text{ cm}^{-2}$ (Ref. 1) and is neglected here. Figure 2 represents the distribution function for the electron population in the first subband calculated for two values of electron sheet concentration N_s . Two separate groups of electrons are readily seen in the first subband: “cool” electrons in the subband bottom and “hot” electrons in high-energy states characterized by the distribution function (4). The inverted population of the high-energy states is formed by cascade-like emission of optical phonons and intrasubband plasmons, whereas the subband bottom states with $k \leq k_F$ are filled mostly due to the one-step events of intersubband plasmon excitation. We would like to emphasize that the latter process effectively fills precisely those states which are the final states for light-emitting transitions¹³ (states with $k \leq k_F$ in the model considered here), restricting to some extent the value of inverted population associated with laser action. This trend becomes more pronounced if the depopulation time, $\tau_{1\text{out}}$, increases. The inset in Fig. 2 shows the occupation number f_0 for the bottom states in the first subband as a function of the electron concentration n_2 , calculated for two different values of depopulation time, $\tau_{1\text{out}}$, namely, 1 and 2 ps.

We now turn to the optical characteristics in the quantum well, which are substantially influenced by the intersubband plasmon spectrum. In a system with normal ordering of

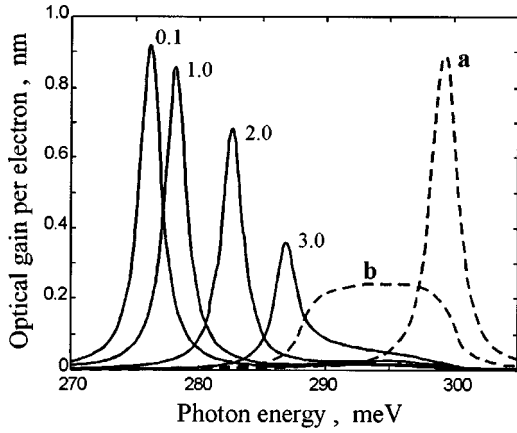


FIG. 3. Downshift and narrowing of the optical gain spectra due to the depolarization effect in a quantum well with inverted subband occupation. Dashed curves represent calculations neglecting the depolarization effect ($\alpha=0$) for two values of electron concentration n_2 : (a) $5 \times 10^{10} \text{ cm}^{-2}$; (b) $4 \times 10^{11} \text{ cm}^{-2}$. Solid curves labeled with the value of tunneling depopulation time $\tau_{1\text{out}}$ (in ps) illustrate the influence of the first-subband bottom filling on the gain spectrum at $n_2=4 \times 10^{11} \text{ cm}^{-2}$. The low-temperature value $\hbar\gamma=1 \text{ meV}$ was taken for the polarization dephasing rate (Ref. 14).

the subband occupation the lightwave field screening by the electron gas leads to an upshift in the energy of the intersubband absorption spectrum.^{4,5} At high electron concentrations the absorption linewidth is considerably narrower than the single particle broadening determined by the nonparabolicity of the subbands.^{14,15} We will show that for a quantum well with inverted subband occupation the depolarization field associated with the nonequilibrium intersubband plasmon excitations $\omega_{\text{pl}}^{(21)}$ leads to a downshift of the emission peak and a corresponding downshift and narrowing of the optical gain spectra. For a two-subband model, following Refs. 14–16 we obtain low-temperature long-wavelength susceptibility $\chi(\omega, q \rightarrow 0)$, which includes the depolarization-field effect under the condition of inverted subband population, and determines the optical gain:

$$g(\omega) = \frac{\omega}{c\sqrt{\kappa_\infty}} \text{Im} \chi(\omega, 0),$$

$$\chi(\omega) = \frac{e^2 z_{12}^2 n_2}{2\pi \Delta_{21} \kappa_0} (1-f_0) \frac{G(\omega)}{1-\alpha G(\omega)}, \quad (5)$$

$$G(\omega) = \frac{\Delta_{21}}{\epsilon_F} \int_0^{\epsilon_F} \frac{\Omega_\epsilon d\epsilon_2}{\Omega_\epsilon^2 - \hbar^2 \omega^2 - 2i\hbar^2 \omega \gamma},$$

$$\alpha = (n_2 - n_0) \frac{2e^2 S}{\Delta_{21} \kappa_0 \kappa} (1-f_0).$$

Here, $\Omega_\epsilon = \Delta_{21} + \epsilon_2 - \epsilon_1$ is the energy separation for a particular “vertical” transition and γ is polarization dephasing rate, which we assume to be a constant.¹⁴ The dipole matrix element z_{12} and the depolarization integral S are also assumed to be k independent; in a two-subband model with infinitely deep quantum well they equal, respectively, $16a/9\pi^2$ and $5a/9\pi^2$. In the case of normal subband occupation, the parameter α in Eq. (5) changes sign and we arrive at the results of Zaluzny¹⁵ and Warburton *et al.*¹⁶ for optical absorption. The factor $(1-f_0)$ describes the effect of the

first-subband bottom filling, which in our model occurs due to the nonequilibrium intersubband plasmon excitation.

In Fig. 3 we show the results of exemplary gain spectra calculations. Taking into account the resonance screening of the light field (solid curves) we obtain a substantial downshift of the gain peak position and the line narrowing analogous to that observed in absorption spectra.¹⁶ The linewidth at the half-maximum level is practically “pinned” at the value $2\hbar\gamma$. This agrees well with the experimental observations of the narrow spontaneous emission linewidth even for high-temperature operating QCL heterostructures.^{9,17} Our results show also the remarkable influence of the lower-subband bottom filling on the gain peak position. The maximum shift of the gain spectrum is achieved at low value of depopulation time $\tau_{1\text{out}} \approx 0.1 \text{ ps}$, which is typical for modern QCL design,¹⁷ while the increase of $\tau_{1\text{out}}$ leads to a more effective filling of the subband bottom (see Fig. 2) and results in substantial decrease of the peak shift.

In conclusion, it is demonstrated that the collective effects in quantum wells with inverted subband occupation differ significantly from those in normal systems. The excitation of intersubband plasmons lowers the energy of the nonequilibrium initial state and opens a new relaxation channel for high-energy electrons in the lower subband. We have shown that the intersubband resonance screening of the lightwave electric field in these systems leads to both narrowing and anomalous downshift of the optical gain spectrum.

The authors would like to thank M. Hybertsen, R. Kazarinov, and V. Gorfinkel for helpful discussions. This work was supported by the U.S. Army Research Office under Grant No. DAG55-97-1-0009.

- ¹S. Das Sarma, in *Hot Carriers in Semiconductor Nanostructures*, edited by J. Shah (Academic, New York), 1996, p. 53.
- ²G. F. Giuliani and J. J. Quinn, *Phys. Rev. B* **26**, 4421 (1982); M. Artaki and K. Hess, *ibid.* **37**, 2933 (1988); W. Harrison, *ibid.* **53**, 12 869 (1996).
- ³S. M. Goodnick and P. Lugli, *Phys. Rev. B* **37**, 2578 (1988); J. H. Smet, C. G. Fonstad, and Q. Hu, *J. Appl. Phys.* **79**, 9305 (1996); S. C. Lee and I. Galbraith, *Phys. Rev. B* **55**, 16 025 (1997).
- ⁴S. J. Allen, D. C. Tsui, and B. Vinter, *Solid State Commun.* **20**, 425 (1976).
- ⁵B. Vinter, *Phys. Rev. B* **15**, 3947 (1977).
- ⁶D. A. Dahl and L. J. Sham, *Phys. Rev. B* **16**, 651 (1977).
- ⁷S. Das Sarma, *Phys. Rev. B* **29**, 2334 (1984).
- ⁸L. Wendler and R. Pechstedt, *Phys. Status Solidi B* **141**, 129 (1987).
- ⁹J. Faist, F. Capasso, D. L. Sivco, A. L. Hutchinson, and A. Y. Cho, *Science* **264**, 553 (1994); J. Faist, F. Capasso, C. Sirtori, D. L. Sivco, A. L. Hutchinson, M. S. Hybertsen, and A. Y. Cho, *Phys. Rev. Lett.* **76**, 411 (1996).
- ¹⁰B. Gelmont, V. Gorfinkel, and S. Liryi, *Appl. Phys. Lett.* **68**, 2171 (1996); V. Gorfinkel, S. Luryi, and B. Gelmont, *IEEE J. Quantum Electron.* **32**, 1995 (1996).
- ¹¹N. C. Constantinou, *J. Phys.: Condens. Matter* **3**, 6859 (1991).
- ¹²M. Kisin, M. Stroschio, G. Belenky, V. Gorfinkel, and S. Luryi, *J. Appl. Phys.* **83**, 4816 (1998).
- ¹³V. F. Elesin and Yu. V. Kopae, *JETP* **81**, 1192 (1995).
- ¹⁴T. Ando, *J. Phys. Soc. Jpn.* **44**, 475 (1978).
- ¹⁵M. Zaluzny, *Phys. Rev. B* **43**, 4511 (1991).
- ¹⁶R. J. Warburton, C. Gauer, A. Wixforth, J. P. Kotthaus, B. Brar, and H. Kroemer, *Superlattices Microstruct.* **19**, 365 (1996).
- ¹⁷C. Sirtori, J. Faist, F. Capasso, D. L. Sivco, A. L. Hutchinson, S. N. G. Chu, and A. Y. Cho, *Appl. Phys. Lett.* **68**, 1745 (1996); C. Gmachi, A. Tredicucci, F. Capasso, A. L. Hutchinson, D. L. Sivco, J. N. Baillargeon, and A. Y. Cho, *ibid.* **72**, 3130 (1998).